Climatic Change (2010) 102:579–593
DOI 10.1007/s10584-009-9704-1

Simulation of organic carbon dynamics at regional scale for paddy soils in China

Xue-Zheng Shi · Ru-Wei Yang · David C. Weindorf · Hong-Jie Wang · Dong-Sheng Yu · Yao Huang · Xian-Zhang Pan · Wei-Xia Sun · Li-Ming Zhang

Received: 4 July 2008 / Accepted: 27 August 2009 / Published online: 10 October 2009

Abstract Accurate simulation of soil organic carbon (SOC) dynamics is vitally important in researching the carbon cycle in terrestrial ecosystems. Especially, the application of SOC model at the regional scale has major implications for regional and global carbon cycling. This paper addresses the regional simulation for SOC in the surface layer (0∼15 cm) of paddy soils in Wuxi and Changzhou, Jiangsu Province, China from 1982∼2000 by linking a model of agro-ecosystem SOC dynamic simulation with GIS data on the basis of 100 × 100 m grids. The dataset includes soil profile descriptions and chemical data of 187 paddy soil samples in the Second National Soil Survey of China in 1982 and 352 paddy soil samples taken in 2000. Soil maps at a scale of 1:50,000 were used for the simulation. Results showed that the area of differences between simulated and observed SOC in 2000 (in the range of −3.6 to 3.6 Mg C ha^{-1}) accounted for 50.6% of the total area. Also, when a 10% and 20% simulated increase, and a 10%, 20% and 30% simulated decrease in harvested crop straw and manure amendments were simulated to test the sensitivity of the model, simulated SOC would range from 10.26 to 50.40 Mg C ha^{-1} with a standard deviation of 1.6 and 2.5, respectively. It is indicated that a key factor controlling SOC is the amount of residue and manure inputs. As for the assessment model suitability based on soil textures, soil types, and parent materials, the model seemed

X.-Z. Shi · R.-W. Yang · H.-J. Wang (✉) · D.-S. Yu · X.-Z. Pan · W.-X. Sun · L.-M. Zhang
State Key Laboratory of Soil and Sustainable Agriculture, Institute of Soil Science, Chinese Academy of Sciences, Nanjing, 210008, China
e-mail: hjwang@issas.ac.cn

R.-W. Yang
Nanjing Xiaozhuang University, Nanjing, 210015, China

D. C. Weindorf
Louisiana State University AgCenter, Baton Rouge, LA 70803, USA

R.-W. Yang · Y. Huang · L.-M. Zhang
College of Resources and Environmental Sciences, Nanjing Agricultural University, Nanjing, 210095, China

to perform better for clayey soils, groundwater-related paddy soils and soils derived from alluvial parent material than for loamy soils, surface water-related paddy soils and soil derived from loess material.

Abbreviations

GIS	Geographic information system
NDVI	Normalized difference vegetation index
RS	Remote sensing
SOC	Soil organic carbon
ST	Soil taxonomy

1 Introduction

Soils represent the most fundamental resource required for agricultural production. Soil organic carbon (SOC) plays an important role in enhancing soil fertility for good agronomic production. An estimated 1,500 Pg of C is held in the form of SOC, which represents 2/3 of the global terrestrial organic carbon pool (Eswaran et al. 1993; Lal et al. 1995). Furthermore, SOC plays a vital role in the global carbon cycle. Even a slight change in the soil carbon pool would cause profound changes in atmospheric CO_2 concentrations. However, soil carbon turnover rates are being accelerated by increased land exploitation and changes in land use (Houghton and Hackler 2003; Wang et al. 2004; Wu et al. 2006; Zach et al. 2006; West and Six 2007; Cui and Graf 2009). Hence, it has become more popular in recent decades to apply dynamic simulation model approaches to SOC change issues. Up to now, more than ten dynamic models have been created to simulate SOC changes such as the RothC (Jenkinson and Rayner 1977), CENTURY (Parton et al. 1988), DNDC (Li et al. 1992a, b), NCSOIL (Molina et al. 1983), DAISY (Mueller et al. 1996), CANDY (Franko et al. 1995), and SOMM (Chertov and Komarov 1997). All these models were tested and compared with data from long-term, on-station experiments.

With continuous improvements to SOC models and the rapid development of computer technology, it is possible to simulate SOC dynamics at the regional scale by using data (taken from a variety of sources including remotely sensed ones) organized in a Geographic Information System (GIS) linked to models. Ardö and Olsson (2003) assessed SOC dynamics during the period 1900–2100 for an area of 512×512 km in the province of Northern Kordofan in semi-arid Sudan by integrating GIS with the CENTURY model and found that SOC decreased from 1900–2000 and would increase from 2000–2100. The maximum potential carbon sink for the period 2000–2100 was estimated to be 17 Mt. Miehle et al. (2006) predicted forest soil carbon dynamics at two different scales ($\sim$0.045 ha plot^{-1} scale and $\sim$100 ha grid^{-1} scale) across Victoria, in south-eastern Australia using the DNDC model and reported that reduced availability of input data at the larger scale would introduce serious prediction errors. Tang et al. (2006) simulated SOC changes in croplands of China in 1998 using the DNDC model. Data used was obtained from 2,473 counties in China and 1:4,000,000 soil maps. The model results showed that SOC for croplands in China would be lost at a rate of 78.89 Tg C y^{-1}. Cerri et al. (2007) linked CENTURY, RothC and the Intergovernmental Panel on Climate Change (IPCC) method with 1:5,000,000 SOTER data to estimate SOC stock changes for the years 2000 and 2030 in the Brazilian Amazon. These three methods used showed a decline in SOC stock for the period studied.

Although considerable work associated with SOC models has been done in recent years, most of the available dynamic models were built for applications in meadow, forest or upland cropland conditions. Not too many comprehensive models were used for paddy soils which are subject to seasonal wetting–drying fluctuations. In China, two models for paddy SOC dynamic simulation associated with paddy soil features have been constructed: one was an agro-ecosystem SOC dynamic model (Huang et al. 2002), the other was a soil organic carbon and nutrient cycling simulation model (SCNC) (Tong et al. 2001). For instance, Shen et al. (2003) succeeded in simulating SOC dynamics of paddy soils in agro-ecosystems of the Jiangsu Province from 1985 to 2000. This allowed for the prediction of the spatial distribution of SOC in 2010 by linking the agro-ecosystem SOC dynamic model with GIS data on the basis of 2,000 × 2,000 m grids. Zhang et al. (2007) estimated soil organic matter dynamics of paddy soils in China from 1980 to 2000 by linking a coupled bio-physical model to a GIS database on the basis of 10 × 10 km grids. However, most dynamic models were only tested or validated with field-scale long-term static observation data due to a lack of available soil data with temporal and spatial variation (Shirato 2005; Wang et al. 2005; Lei et al. 2006) except for some preliminary studies by Shen et al. (2003). Since these models have not yet been validated by regional scale data, uncertainty exists when they are applied to simulations of SOC dynamics at regional scales. Additional uncertainty appears when these simulations are applied without full consideration of soil types and spatial heterogeneity of soil attributes.

Paddy soils are a group of anthropogenic soils with a long history of rice cultivation under irrigation, and unique soil type in China's taxonomy (Gong 1999). The total area of paddy soils in China reached 30 Mha in the mid-1980s (23% of the world's total irrigated lands). Paddy soils produce one-quarter of grains for China's market (Gong 1999). The purposes of this paper are to simulate SOC changes of paddy soils that occur over 18 years (1982–2000) in Wuxi and Changzhou of Jiangsu Province, China by means of the agro-ecosystem SOC dynamics model and to evaluate the model suitability for paddy soils. The model was run based on the 1:50,000 soil database with 100 × 100 m grids. It compared simulation results with the spatial distribution of SOC measurements from 352 sampling sites of paddy soils in 2000, as a means of model validation and assessment at the regional scale. This data will allow for further modification of the dynamic model as well as a theory base for regional-scale SOC prediction.

2 Materials and methods

2.1 Study area

The Taihu region, a common area for rice cultivation, is located in the middle and lower reaches of the Yangtze River paddy soil region of China (Li 1992). Wuxi and Changzhou are located in the Taihu region, in the southern Jiangsu Province (119°08′ ∼120°56′ E, 31°07′ ∼32°04′ N), covering a total area of 9,030 km^2 (Fig. 1). In the study area, paddy soils cover about 80% of the territory (Yang et al. 2006). The paddy soils are derived mostly from loess, alluvium and lacustrine deposits

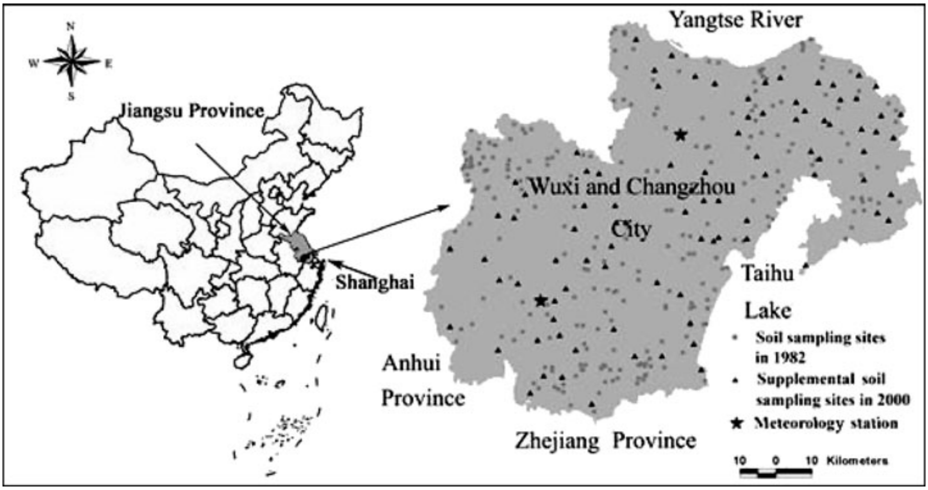

Fig. 1 Location of the study area and a map of soil sampling sites and meteorology stations in the Jiangsu Province, China

and are classified in the following subgroups as referenced to US Soil Taxonomy (ST) (Soil Survey Staff 1994): Hydromorphic (Typic Epiaquepts), Submergenic (Typic Endoaquepts), Bleached (Typic Epiaquepts), Gleyed (Typic Endoaquepts), Percogenic (Typic Epiaquepts), and Degleyed (Typic Endoaquepts) (Shi et al. 2006). Rice and corn are typically planted from June to October and wheat and rapeseed are planted from November to May annually under minimum or no-tillage practices in the region (Shen et al. 2003). Mean annual precipitation is about 1,100 mm. During the dry season, ground water levels and precipitation are 80 cm and 30 mm, respectively (Xu et al. 1980).

2.2 Data sources

Soil attribute data such as SOC, bulk density and textures were retrieved from the 1:50,000 soil database of Wuxi and Changzhou as model initial values. The surface layer (0~15 cm) data from 187 soil profiles were linked to spatial databases using the Pedological Knowledge Based (PKB) method (Shi et al. 2004; Zhao et al. 2005, 2006). Both soil attributes and spatial data were obtained from local soil survey reports during the Second National Soil Survey of China in 1982. Additional soil data for model validation was obtained from the surface samples (0~15 cm) of 352 paddy soils sampled at the same sites in 2000 (Shi et al. 2004).

Meteorological data was collected from various stations of the National Meteorological Bureau of China, which included daily maximum and minimum air temperatures, sunshine duration, and precipitation during the period of 1982 to 2000. Based on the analysis of original meteorological data, mean temperature, sunshine and precipitation were calculated, which were 16.3 °C, 5.23 h and 31.8 mm, respectively. Annual yields for rice, wheat, corn and rape from 1982 to 2000 were obtained from Rural Economic Data of Jiangsu Province (Statistical Bureau of Jiangsu Province 1982~2000). Normalized difference vegetation index (NDVI) data

Fig. 2 Conceptual explanation for modeling SOC dynamics. Note: *F* refers to the fraction of initial labile-C of the added organic matter, and is determined by the initial content of total nitrogen and lignin in the external input

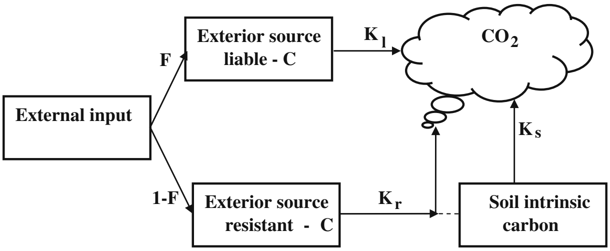

from April and August, 2003, and April and August, 2004 came from the MODIS Satellite Remote Sensing Receiving Station at Wuhan University.

2.3 Model and parameters

The agro-ecosystem SOC dynamic model for simulating farmlands, especially paddy soils, was created by Huang et al. (2002). A conceptual explanation for modeling SOC dynamics is presented in Fig. 2 (Yu et al. 2006). After exterior source carbon is inputted into soil, one part of carbon decomposes to CO_2, while the other part is converted into soil organic matter-carbon. It is generally recognized that the carbon of organic matter such as plant residue, crop straw, green manure and animal manure consists of two components, labile and resistant C. The labile-C includes mainly sugars, proteins and starches. The resistant-C refers to more recalcitrant compounds like lignin.

The model was represented by a differential Eq. 1 as follows (Huang et al. 2002; Shen et al. 2003; Yu et al. 2006):

$$dC_i/dt = K_i \times f_T \times f_W \times f_S \times C_i (i = l, r, s) \quad (1)$$

where i represents a series of carbon fractions: exterior source labile-C (l), exterior source resistant-C (r), soil intrinsic carbon (s); C_i represents the amount of soil carbon of fraction i at time t, K_i is the first-order decay rate constant (months^{-1}) of fraction i; and f_T, f_W, and f_S represent functions of soil temperature, water and clay contents, respectively.

Huang et al. (1998 and 2002) defined the temperature factor function (f_T) as Eqs. 2 and 3:

$$f_T = Q_{10}^{(Ts-10)/10} \quad (2)$$

$$Ts = 4.4 + 0.75T_a \quad (3)$$

where Ts and T_a represent soil and air temperature (°C), respectively and Q_{10} is the temperature coefficient of soil respiration with a value of 2.0.

The effect of soil water on organic carbon decomposition was defined by Huang et al. (2002) and Shen et al. (2003) in Eqs. 4 and 5:

$$f_W = 0.49EXP\left(3.88W - 5.40W^2\right) \quad (4)$$

$$W_i = W_{i-1} + \left(R_i - E_i\right) \quad (5)$$

where f_W represents the relative value of decomposition without considering water percolation and ground runoff, W is the soil water content (gravimetric percentage); W_i and W_{i-1} are the soil water content (millimeters) at time i and i-1, respectively; R_i and E_i are precipitation (millimeters) and evapotranspiration (millimeters) at time i. E_i was computed using the Thornthwaite equation (Jenkinson 1988).

The effect of soil texture on organic carbon decomposition was defined by Huang et al. (2002) in Eq. 6:

$$f_S = 1 - 0.26\mathrm{Clay} \tag{6}$$

where f_S refers to the relative effect of soil clay content on organic carbon decomposition (percent). The clay content (percent) represents particles with a diameter of less than 0.002 mm.

Shen et al. (2003) simulated the initial proportion of the labile-C in the exterior source organic carbon (f_m) as Eq. 7:

$$f_m = (150 + 1.496\mathrm{N} - 0.572\mathrm{L})/100 \tag{7}$$

where N represents the initial content of total nitrogen (grams per kilogram) in plant residues, and L, the initial content of lignin (grams per kilogram) in plant residues (Huang et al. 2003).

The amount of residue retention was estimated based on the crop yield, the ratio of straw to grain yield, and straw incorporated into the soil (Shen et al. 2003; Huang et al. 2007) (Table 1). The amount of animal manure application was approximately 2.25 t ha^{-1} $year^{-1}$ (Shen et al. 2003). In order to obtain an initial value of the resistant-C (*e.g.* lignin which has a half-life of 2 to 5 years) from crop residue retention and animal manure amendments before 1982, the model was initially run from 1971 to 1982 (Zhang et al. 2007). The first-order decay rates (K_l, K_r and K_s) were defined as C decomposition monthly in the exterior source labile-C fraction, exterior source resistant-C fraction and soil intrinsic carbon fraction for sandy soils when f_S, f_W and f_T were all equal to 1, respectively. K_l, K_r and K_s were estimated at 0.38, 0.012 and 0.001 ($months^{-1}$) respectively, using a method by Huang et al. (2002).

2.4 SOC storage calculation and soil texture grouping

Soil organic carbon storage was calculated using Eq. 8 (Batjes 2005, 2006):

$$P_{oc}\,(\mathrm{tC}) = \mathrm{SOC} \times \gamma \times \mathrm{H}/100 \times (1 - \delta_{2mm}\%) \times \mathrm{S} \tag{8}$$

where P_{oc} is SOC storage (kilograms) in the surface layer (0~15 cm), SOC is soil organic carbon (grams per kilogram), γ is soil bulk density (grams per cubic

Table 1 Parameters used for estimating the amount of residue retention

Crop	The ratio of the straw to grain yield	The ratio of straw incorporated into soil (%)	The ratio of root to shoot (%)
Rice	1.31	27	10
Wheat	1.77	30	10
Corn	1.27	10	10
Rapeseed	2.99	35	10

Sources: Zhang and Zhu (1990), Shen et al. (2003), Huang et al. (2007)

centimeter), H is layer thickness (centimeters), $\delta_{2\ mm}$ is gravel (>2 mm) content (%), and S is surface area of the study area (kilometer squared). In this study, γ was fixed as 1.2 g cm^{-3} (an averaged value), H = 15 cm, and $\delta_{2\ mm} = 0$ due to the absence of gravel in the surface of paddy soils. Also, S = 5,920 km^2, calculated by the sum of paddy soil polygons from the 1:50,000 soil database of Wuxi and Changzhou.

Soil particles were divided into three categories: sand (2∼0.05 mm), silt (0.05∼0.002 mm) and clay (<0.002 mm), according to the USDA Soil Survey Manual (Soil Survey Staff 2003). Soil textural classes were then assigned using the USDA textural triangle. In this study, only SOC in loamy and clayey soils was considered in the simulation model due to the limited extent of sandy soils (4.7%) in the study area.

2.5 Software and calculation

Using ARC/INFO software (version 8.3), a 100 × 100 m grid system was created with identical left-bottom coordinates (1,320,000, 3,397,000 m) and soil attribute datasets (such as SOC, clay content and bulk density) from the 1:50,000 soil databases of Wuxi and Changzhou. Similarly, a 100 × 100 m grid system of crop yield data based on yield statistics was also created by inputting data into an attribute table, with NDVI data as the ratio coefficient. Regional distribution of the climatic data (including mean monthly air temperature, sunshine duration, and precipitation) was integrated by treating those data with an inverse distance weighted (IDW) interpolation. Then, all ASCII files were created from grid data by running ARC/INFO software. The ASCII data files were inputted into a model code program written with Visual Basic 6.0. Finally, SOC was simulated by running the model code program in a monthly stepwise fashion with grid positions as the basic simulation units. Spatial distribution of the SOC for each grid was displayed by loading it into ArcMap.

3 Results and discussion

3.1 Regional SOC distribution of paddy soil and its dynamics features

A map of SOC for paddy soils at surface layers (0∼15 cm) in the study area in 1982 was constructed on the basis of observed SOC data from the finished 1:50,000 soil database (Yang et al. 2006) (Fig. 3a). Also, a corresponding SOC map in 2000 was constructed based on the data at the surface layers (0∼15 cm) of 352 paddy soil samples taken in the study area in 2000 (Fig. 3b). Then, a map of spatial SOC change during the 18 years (1982∼2000) was formed by overlapping the two aforementioned maps (Fig. 3c). Figure 3a shows that the observed SOC in 1982 varied from 6.66 to 33.12 Mg C ha^{-1}, and the area with SOC of 9.0∼27.0 Mg C ha^{-1} accounted for 78.0% of the total study area. By comparison, Fig. 3b shows that observed SOC in 2000 varied from 8.10 to 60.84 Mg C ha^{-1}, and the area with SOC of 18.0∼45.0 Mg C ha^{-1} accounted for 84.8% of the entire area. Thus, the range of observed SOC in 2000 is wider than that in 1982, and the content of observed SOC in 2000 is higher than that in 1982 in most of the study area. More specifically, Fig. 3c indicates that the area with increased SOC in 2000 compared to that in 1982 accounted for 92.1% of the total paddy soils in the study area. Decreases in SOC from 1982 to 2000 covered

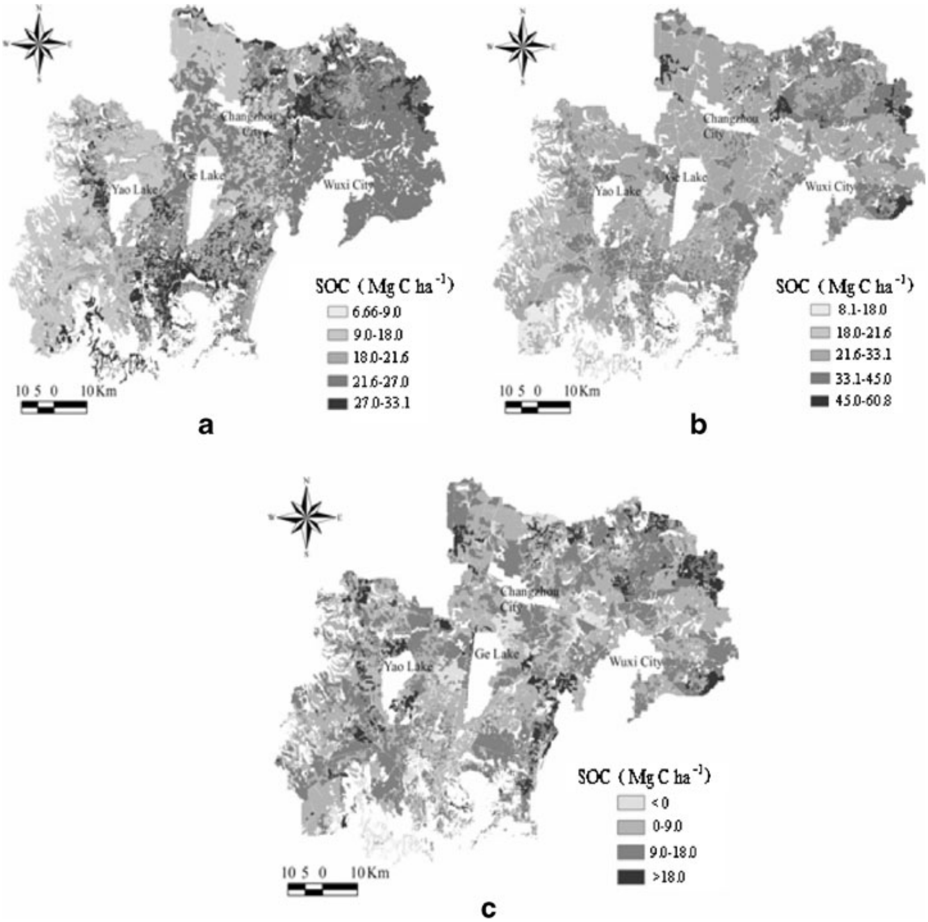

Fig. 3 Spatial variability of observed SOC for paddy soils in Jiangsu Province, China for **a** 1982, **b** 2000, and **c** spatial variability of changes in observed SOC between 1982 and 2000

only 7.9% of the total area. Moreover, the areas with SOC increases in the range of 0~9.0 Mg C ha^{-1} accounted for about 46.3% and areas with SOC increases in the range of 9.0~18.0 Mg C ha^{-1} accounted for 40.4%.

3.2 Comparison between simulated and observed SOC for paddy soil in 2000

Regional SOC was simulated by running the model from 1982–2000. SOC simulations were produced by overlapping and running every grid with data factors of temperature, climate, crop yield and soil texture. The observed SOC of paddy soils in 1982 represented the initial SOC for the model simulation while the observed SOC in 2000 served as the model validation reference. Figure 4a shows the map of simulated paddy SOC in 2000. A map of the change between the simulated and observed SOC in 2000 (Fig. 4b) was generated by overlapping the map of simulated SOC in 2000 with that of observed SOC in the same year in corresponding grids. Figure 4a shows a

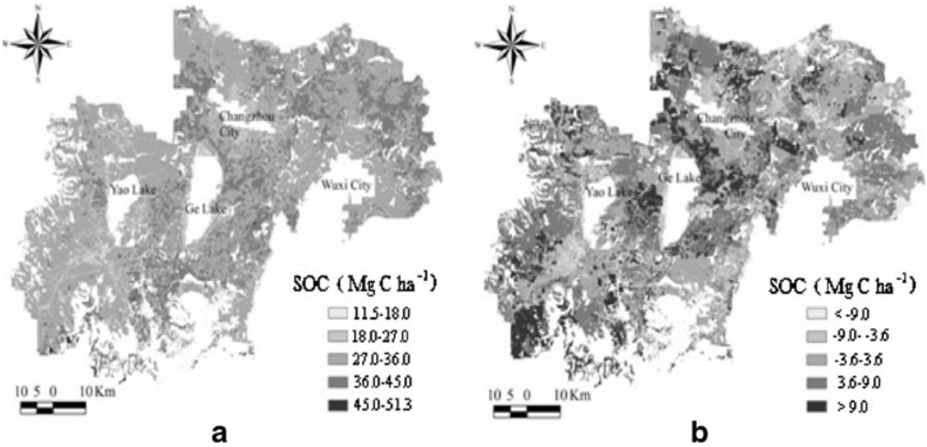

Fig. 4 Spatial variability of SOC for paddy soils in Jiangsu Province, China for **a** simulated SOC levels for paddy soils in 2000 and **b** the difference between observed and simulated SOC levels for paddy soils in 2000

map of simulated SOC in 2000, with a narrower SOC range (11.52~51.30 Mg C ha^{-1}) than the observed one (8.10~60.84 Mg C ha^{-1}) in the same year. Furthermore, the proportion of the simulated SOC and observed SOC with different content ranges was shown in Table 2. The simulated SOC had a more concentrated range than did the observed SOC (in the range of 21.6~45.0 Mg C ha^{-1}), which included the majority of the total area. Figure 4b shows the spatial heterogeneity of the change between simulated and observed paddy SOC in 2000. The map shows that paddy soil areas with a change of >9.0 Mg C ha^{-1} accounted for 3.2% of the total area, <−9.0 Mg C ha^{-1} representing 10.4% of the area, with the remaining 86.4% displaying a change range of −9.0~9.0 Mg C ha^{-1}. For paddy soil areas with an even narrower range (−3.6~3.6 Mg C ha^{-1}), the areas of change between simulated and observed SOC constituted 50.6% of the total study area. Thus, simulated SOC levels were close to those observed in many cases.

The frequency distribution of residual errors between simulated and observed SOC in 2000 was analyzed (Fig. 5). Figure 5 indicates that the frequency distribution of the residual errors followed a normal distribution, which made a sense from statistical perspective. The percentage of the residual errors in the range of $\leq \pm 3.6$ Mg C ha^{-1} accounted for 49.9% of the total data. In addition, simulated

Table 2 Proportion of the simulated SOC and observed SOC with the different SOC content range

SOC content range (Mg C ha^{-1})	8.1–9.0 (%)	9.0–18.0 (%)	11.52–18.0 (%)	18.0–21.60 (%)	21.60–27.0 (%)
Simulated SOC	–	–	0.62	0.88	4.39
Observed SOC	0.02	2.98	–	6.01	27.0
	27.0–33.12 (%)	33.12–36.0 (%)	36.0–45.0 (%)	45.0–51.3 (%)	45.0–60.84 (%)
Simulated SOC	37.7	31.1	25.0	0.31	–
Observed SOC	37.0	12.1	12.7	–	2.19

– no value (it is different between simulated SOC content range and observed SOC one)

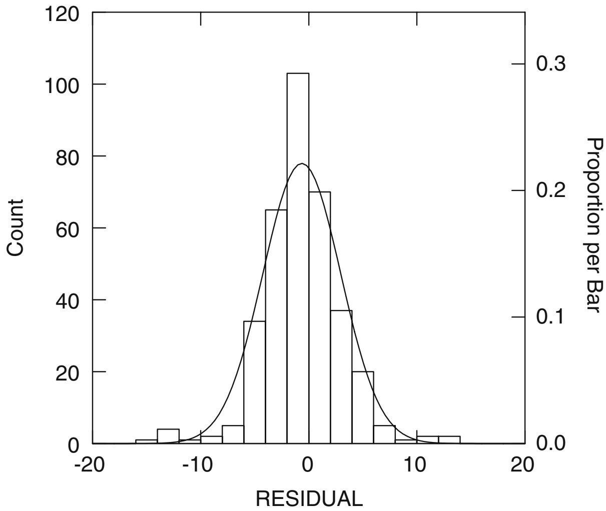

Fig. 5 The frequency distribution of changes between observed and simulated SOC in 2000. Note: Residual = observed SOC − simulated SOC

values (31.16 ± 3.78 Mg C ha^{-1}) were relatively close to observed values (29.99 ± 6.50 Mg C ha^{-1}) at a spatial scale. The former was generally 3.9% higher than the latter. Therefore, the results of residual errors were consistent with the statistical results from the soil map.

Simulation results were further assessed by comparing surface layer paddy SOC storage. Inputting observed and simulated SOC values of corresponding grids into Eq. 8, SOC storage was calculated. Results showed that the simulated SOC storage in the surface layers (19.7 Tg) was 1.9 Tg higher than the observed value (17.8 Tg). Thus, the relative error of the simulated SOC storage was about 10.7% when referenced to the observed value.

3.3 Sensitivity analysis for simulation results

Yu et al. (2006) reported that the sensitive significance of the agro-ecosystem SOC model for dynamic simulation of input parameters descended in order of temperature, quantity of incorporated organic carbon, soil pH, initial value of resistant organic matter, precipitation and soil clay. However, the quantity of incorporated organic carbon impacted by human activities has more uncertainty than other factors. Hence, a 10% and 20% simulated increase, and a 10%, 20% and 30% simulated decrease in biomass of crop straw and manure amendments were simulated to test the sensitivity of the model. The estimates of SOC were then calculated based on the aforementioned conditions and the spatial datasets of residue retention and organic manure amendment. Results showed that simulated SOC ranged from 10.26 to 50.40 Mg C ha^{-1} with standard deviations of 1.6 and 2.5, respectively. As C inputs in the simulation are altered, the number of 'poor fit points' varies from 66 to 88 (Table 3). 'Poor fit points' were identified using the difference between simulated and observed SOC, where points fall outside the range of −9.0 to 9.0 Mg C ha^{-1}. Conversely, good fit points fall inside the range of −9.0 to 9.0 Mg C ha^{-1}. As the simulation varies, some good fit points become poor fit points and some poor fit points become good fit points. It was discovered that reducing C input can improve

Table 3 List of poor fit points comparing simulated and observed SOC in 2000

Variation of residue and manure inputs (%)	+20%	+10%	Baseline	−10%	−20%	−30%
Total poor fit points	88	78	74	70	66	74
Poor fit changed to good fit	3	6	N/A	24	29	30
Good fit changed to poor fit	17	10	N/A	20	21	30

Variation of residue and manure inputs (%)
+10%, +20% 10% and 20% increase in harvest crop straw and the manure amendment, *−10%, −20%, −30%* 10%, 20% and 30% decrease in harvest crop straw and the manure amendment

simulation models. For the tested simulations, a 20% decrease was the best fit for model simulation because the differences were the smallest between simulated and observed SOC causing an overall increase in good fit points. Unfortunately, various input rates from fields have not been received to validate the prediction of SOC with increasing or decreasing amounts of amended crop residues and animal manures. However, a key factor controlling SOC is the amount of residue retention and manure amendment. Further effort should focus on getting more detailed information about the residue retention and manure amendments both spatially and temporally to improve the simulation.

3.4 Assessment model suitability

Presently, internationally popular SOC dynamic simulation models are usually applied for specific land-use types only to pursue improved simulation precision (Chertov and Komarov 1997; Smith et al. 1997). Despite single land-use status, paddy SOC heterogeneity was found in the study area due to varied paddy soil textures, subgroups and parent materials (Li 1992; Wang et al. 2003; Liu et al. 2006; Yu et al. 2007). If model precision is to be improved, SOC simulation should be based on specific combinations of various soil textures, subgroups and parent materials.

The majority of paddy soils in the area were clayey or loamy. As such, correlation analysis between observed and simulated SOC levels was conducted separately in clayey (Fig. 6a) and loamy (Fig. 6b) paddy soils to assess simulation results. The simple correlation coefficient (r) between simulated and observed SOC levels was 0.60 for clayey soils and 0.55 for loamy soils.

Paddy soils in the study area were derived mainly from loess, Yangtze-river alluvium and lacustrine deposits. Simulated and observed SOC storage, calculated with Eq. 8, in paddy soil surface layers in 2000 for various parent materials and subgroups are listed in Table 4.

Table 4 clearly shows that the relative errors of the simulated SOC storage with reference to those observed vary remarkably with subgroups of paddy soil but less remarkably with parent materials. Relative errors for the Hydromorphic, Submergenic and Bleached paddy soils were more than 10% greater than those for the Gleyed, Percogenic and Degleyed paddy soils. In particular, the relative errors for the Degleyed and Gleyed paddy soils were less than 1%. In terms of parent materials, the relative error for soils developed on lacustrine deposits was slightly lower than those on loess and Yangtze-river alluvium (Table 4). The model provided a good fit to the simulation of SOC in the Degleyed and Gleyed paddy soils due to the accelerated accumulation and difficult decomposition of SOC in the clayey soils

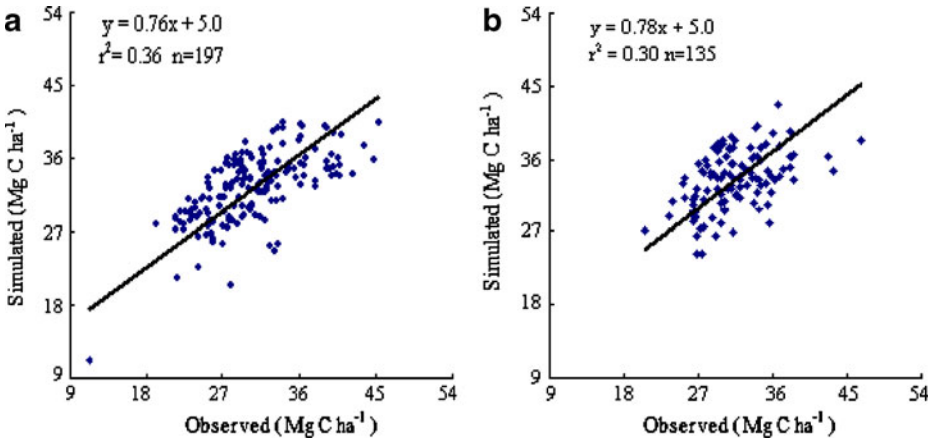

Fig. 6 Correlation analysis of simulated and observed SOC levels in clayey soil (**a**) and loamy soil (**b**) in the study area in 2000

(clay contents 20~50%) formed in lacustrine deposits. This resulted in fewer errors for the simulated SOC with respect to associated observed values. However, lower simulation precisions were found when the model was applied to Hydromorphic, Submergenic and Bleached paddy soils due to parent material-related variation and complex textural variation often characterized by sharp alterations of sand and clay (Li 1992). In addition, despite similarities in hydrology and parent materials for both the Hydromorphic and Percogenic paddy soils, different simulation results were found between the two soil types due to some other influencing factors such as the uncertainties of SOC prediction related to regional simulation (Zhao et al. 2005, 2006).

Table 4 Simulated and observed SOC storage in surface layers of paddy soils for various subgroups and parent materials in Wuxi and Changzhou, China

Paddy soil subgroups	Simulated SOC storage (Tg)	Observed SOC storage (Tg)	Relative error (%)	Parent materials	Simulated storage (Tg)	Observed SOC storage (Tg)	Relative error (%)
Hydromorphic[a]	8.38	7.41	13.1	Loess	9.53	8.53	11.7
Submergenic[b]	1.23	1.04	18.3				
Bleached[a]	6.48	5.68	14.1	Yangtze-river alluvium	5.65	5.09	11.0
Gleyed[b]	0.31	0.31	0.1				
Percogenic[a]	1.22	1.19	2.5	Lacustrine deposits	4.55	4.15	9.6
Degleyed[b]	2.11	2.12	−0.5				

[a]Typic Epiaquepts (Soil Survey Staff 1994)
[b]Typic Endoaquepts (Soil Survey Staff 1994)

4 Conclusions

The regional soil organic carbon dynamics of paddy soils in Wuxi and Changzhou, China were simulated during an 18-year period (1982~2000) using a 100 × 100 m grid based on an agro-ecosystem SOC dynamic simulation model. Results showed that the area of differences between simulated and observed SOC in 2000 (in the range of −3.6 to 3.6 Mg C ha^{-1}) accounted for 50.6% of the total area. This indicates that simulated SOC closely reflected observed SOC in the study area as a whole. When a 10% and 20% simulated increase, and a 10%, 20% and 30% simulated decrease in harvest crop straw and manure amendments were tested, results showed that simulated SOC ranged from 10.26 to 50.40 Mg C ha^{-1} with standard deviations of 1.6 and 2.5, respectively. A key factor controlling SOC is the amount of residue and manure inputs. The model can simulate well the possibility of increasing residue retention and manure amendments in practice in the study region. To assess its suitability based on soil textures, soil types, and parent materials, the model seemed to be better for clayey soil, groundwater-related paddy soil and alluvial parent material than for loamy soil, surface water-related paddy soil and loess material. Regional SOC was simulated directly and simulated SOC was compared with observed SOC at the regional scale, providing data for further research about sector approaches to improve regional carbon budgets (Smith et al. 2008).

Acknowledgements We gratefully acknowledge the supports from the National Natural Science Foundation of China (No. 40621001), the National Basic Research Program of China (No. 2007CB407206) and the Frontier Project of the Chinese Academy of Sciences (No. ISSASIP0715).

References

Ardö J, Olsson L (2003) Assessment of soil organic carbon in semi-arid Sudan using GIS and the CENTURY model. J Arid Environ 54:633–651
Batjes NH (2005) Organic carbon stocks in the soils of Brazil. Soil Use Manage 21:22–24
Batjes NH (2006) Soil carbon stocks of Jordan and projected changes upon improved management of croplands. Geoderma 132:361–371
Cerri CEP, Easter M, Paustian K, Killian K, Coleman K, Bernoux M, Falloon P, Powlson DS, Batjes NH, Miline E, Cerri CC (2007) Predicted soil organic carbon stocks and changed in the Brazilian Amazon between 2000 and 2030. Agric Ecosyst Environ 122:58–72
Chertov OG, Komarov AS (1997) SOMM—a model of soil organic matter dynamics. Ecol Model 94:177–189
Cui XF, Graf HF (2009) Recent land cover changes on the Tibetan Plateau: a review. Clim Change 94:47–61
Eswaran H, Berg EVD, Reich P (1993) Organic carbon in soil of the world. Soil Sci Soc Am J 57:192–194
Franko U, Oelschlagel B, Schenk S (1995) Simulation of temperature-, water-, and nitrogen dynamics using the model CANDY. Ecol Model 81:213–222
Gong ZT (1999) Chinese soil taxonomic classification (In Chinese). China Science, Beijing, pp 5–215
Houghton RA, Hackler JL (2003) Sources and sinks of carbon from land-use change in China. Global Biogeochem Cycles 17(2):1034–1052
Huang Y, Liu SL, Shen QR, Zong LG (2002) Model establishment for simulating soil organic carbon dynamics. Agric Sci China 1(3):307–312
Huang Y, Sass RL, Fisher FM (1998) A semi-empirical model of methane emission from flooded rice paddy soils. Global Change Biol 4:247–268
Huang Y, Shen Y, Zhou M, Ma RS (2003) Decomposition of plant residue as influenced by its lignin and nitrogen (In Chinese). Acta Phytoecol Sin 27(2):183–188

Huang Y, Zhang W, Sun WJ, Zheng XH (2007) NPP primary production of Chinese croplands from 1950 to 1999. Ecol Appl 17(3):692–701
Jenkinson DC (1988) The turnover of organic matter in soil. In: Wild A (ed) Soil conditions and plant growth [M]. Longman, Harlow, pp 564–607
Jenkinson DS, Rayner JH (1977) The turnover of soil organic matter in some of the Rothamsted classical experiments. Soil Sci 123:298–305
Lal R, Kimble J, Levine E, Whitman C (1995) World soils and greenhouse effect: an overview. In: Lal R, Kimble J, Levine E, Stewart BA (eds) Soils and global change. CRC. Boca Raton, pp 27–43
Lei HJ, Li BG, Bai YL, Huang YF, Lü YZ, Li GT (2006) Modeling soil organic matter dynamics under intensive cropping systems on the Huang-Huai-Hai Plain of China. Pedosphere 16(4):409–419
Li C, Frolking S, Frolking TA (1992a) A model of nitrous oxide evolution from soil driven by rainfall events: I. Model structure and sensitivity. J Geophys Res 97:9759–9776
Li C, Frolking S, Frolking TA (1992b) A model of nitrous oxide evolution from soil driven by rainfall events: II. Model applications. J Geophys Res 97:9777–9783
Li QK (ed) (1992) Paddy soil in China (In Chinese). Science, Beijing
Liu QH, Shi XZ, Weindorf DC, Yu DS, Zhao YC, Sun WX, Wang HJ (2006) Soil organic carbon storage of paddy soils in China using the 1:1,000,000 soil database and their implications for C sequestration. Global Biogeochem Cycles 20:GB3024. doi:10.1029/2006GB002731
Miehle P, Livesley S, Li CS, Feikema P, Adams M, Arndt S (2006) Quantifying uncertainty from large-scale model predictions of forest carbon dynamics. Global Change Biol 12:1421–1434
Molina JAE, Clapp CE, Shaffer MJ, Chichester FW, Larson WE (1983) NCSOIL, a model of nitrogen and carbon transformations in soil: description, calibration and behavior. Soil Sci Soc Am J 47:85–91
Mueller T, Jensen LS, Hansen S, Nielsen NE (1996) Simulating soil carbon and nitrogen dynamics with the soil–plant–atmosphere system model DAISY. In: Powlson D, Smith P, Smith JU (eds), Evaluation of soil organic matter models using existing long-term datasets. NATO ASI series I, vol. 38. Springer, Heidelberg, pp 275–282
Parton WJ, Stewart JWB, Cole CV (1988) Dynamics of C, N, P and S in grassland soils: a model. Biogeochem 5:109–131
Shen Y, Huang Y, Zong LG, Zhang W, Xu M, Liu LW (2003) Simulation and prediction of soil organic carbon dynamics in Jiangsu Province based on model and GIS techniques. Agric Sci China 2(9):1007–1013
Shi XZ, Yu DS, Warner ED (2004) Soil database of 1:1,000,000 digital soil survey and reference system of the Chinese Genetic Soil Classification System. Soil Survey Hor 45(4):129–136
Shi XZ, Yu DS, Warner ED, Sun WX, Petersen GW, Gong ZT, Lin H (2006) Cross-reference system for translating between genetic soil classification of China and soil taxonomy. Soil Sci Soc Am J 70:78–83
Shirato Y (2005) Testing the suitability of the DNDC model for simulating long-term soil organic carbon dynamics in Japanese paddy soils. Soil Sci Plant Nutr 51(2):183–192
Smith P, Nabuurs GJ, Janssens IA, Reis S, Marland G, Soussana JF, Christensen TR, Heath L, Apps M, Alexeyev V, Fang JY, Gattuso JP, Guerschman JP, Huang Y, Jobbagy E, Murdiyarso D, Ni J, Nobre A, Peng CH, Walcroft A, Wang SQ, Pan YD, Zhou GS (2008) Sectoral approaches to improve regional carbon budgets. Clim Change 88:209–249
Smith P, Smith JU, Powlson DS, McGill WB, Arah JRM, Chertov OG, Coleman K, Franko U, Frolking T, Parton WJ, Thornley JHM, Whitmore AP (1997) A comparison of the performance of nine soil organic matter models using datasets from seven long-term experiments. Geoderma 81:153–225
Soil Survey Staff (1994) Keys to soil taxonomy. 6th ed. U.S. Gov. Print. Office, Washington, DC
Soil Survey Staff (2003) Soil survey manual. U.S. Gov. Print. Office, Washington, DC
Statistical Bureau of Jiangsu Province (ed) (1982∼2000) Rural economic data of Jiangsu Province. (In Chinese). Jaingsu Statistics, Nanjing
Tang HJ, Qiu JJ, Ranst EV, Li CS (2006) Estimations of soil organic carbon storage in cropland of China based on DNDC model. Geoderma 134:200–206
Tong CL, Wu JS, Guo SL, Xiang WS, Liu SL (2001) The study and development of SCNC model on soil organic carbon turnover. Comput Agric 12:10–12 (In Chinese.)
Wang SQ, Liu JY, Rui GR, Pan YY, Chen QM, Li KR, Li JY (2004) Effects of land use change on the storage of soil organic carbon: a case study of the Qianyanzhou forest experimental station in China. Clim Change 67:247–255

Wang SQ, Tian HQ, Liu JY, Pan SF (2003) Pattern and change of soil carbon storage in China: 1960s–1980s. Tellus 55B:416–427

Wang XB, Cai DX, Hoogmoed WB, Oenema O, Perdok UD (2005) Scenario analysis of tillage, residue and fertilization management effects on soil organic carbon dynamics. Pedosphere 15(4):473–483

West TO, Six J (2007) Considering the influence of sequestration duration and carbon saturation on estimates of soil carbon capacity. Clim Change 80:25–41

Wu CY, Chen Y, Wang JY, Wang SJ (2006) Estimation of turnover and equilibrium of soil organic matter using a mathematical approach. Pedosphere 16(5):634–645

Xu Q, Lu YC, Liu YC, Zhu HG (1980) The paddy soil of Taihu region in China. Shanghai Sci. and Technol., Shanghai

Yang RW, Shi XZ, Yu DS, Huang Y, Xu M, Pan XZ, Jin Y (2006) Spatial heterogeneity of soil properties and there affecting factors—a case study based on 1:50,000 database in Wuxi and Changzhou, Jiangsu province, China. Acta Pedol Sin 43(3):369–375. (In Chinese)

Yu DS, Shi XZ, Wang HJ, Sun WX, Warner ED, Liu QH (2007) National scale analysis of soil organic carbon storage in China based on Chinese soil taxonomy. Pedosphere 17(1):11–18

Yu YQ, Huang Y, Zhang W (2006) Modeling farmland soil organic carbon dynamics in eastern China: model validation and sensitivity analysis (In Chinese). Geog Geo-Inform Sci 22(6):83–88

Zach A, Tiessen H, Noellemeyer E (2006) Carbon turnover and carbon-13 natural abundance under land use change in semiarid savanna soils of La Pampa, Argentina. Soil Sci Soc Am J 70:1541–1546

Zhang FC, Zhu ZH (1990) Harvest index for various crops in China. Sci Agric Sin 23(2):83–87 (In Chinese)

Zhang W, Yu YQ, Sun WJ, Huang Y (2007) Simulation of soil organic carbon dynamics in Chinese rice paddies from 1980 to 2000. Pedosphere 17(1):1–10

Zhao YC, Shi XZ, Weindorf DC, Yu DS, Sun WX, Wang HJ (2006) Map scale effects on soil organic carbon stock estimation in north China. Soil Sci Soc Am J 70:1377–1386

Zhao YC, Shi XZ, Yu DS, Pagella TF, Sun WX, Xu XH (2005) Soil organic carbon density in Hebei Province, China: estimates and uncertainty. Pedosphere 15(3):293–300